

Estimating basal friction in accretionary wedges from the geometry and spacing of frontal faults

Bertram Schott^{a,*}, Hemin A. Koyi^b

^a *Theoretical Geophysics, Utrecht University, P.O. box 80021, 3508 TA Utrecht, The Netherlands*

^b *Department of Earth Sciences, Tectonics and Geodynamics, Uppsala University, Villav. 16, S-75236 Uppsala, Sweden*

Received 29 May 2001; received in revised form 25 September 2001; accepted 4 October 2001

Abstract

Elastic theory applied to the deformation in accretionary wedges is used to calculate the condition for slip along an active frontal fault and the basal décollement. The equations for calculating the stresses can be solved for the coefficient of basal friction in the situation of the formation of a new frontal thrust fault. This allows us to calculate the efficient coefficient of basal friction, which includes the weakening effect of pore-fluid pressure, from geometric parameters and material properties only. The geometric parameters, like fault dip and layer thickness, can be derived from high-resolution seismic cross-sections. Application of our analysis to the Makran and the Nankai accretionary wedge allows us to estimate the upper limit of the effective coefficient of basal friction, $\mu_b \approx 0.16$ and $\mu_b \approx 0.2$, in these two areas respectively. © 2001 Elsevier Science B.V. All rights reserved.

Keywords: accretionary wedges; friction; imbricate tectonics; thrust faults

1. Introduction

There are many theoretical models of the deformation of accretionary wedges: one group are the either non-cohesive [1,2] or cohesive [2–4] Coulomb wedge models; another group are the elastic wedge models [5,6], and the models of plastic deformation [7,8]. All these types of models have been applied to nature and laboratory experiments, in an attempt to improve our understanding of accretionary wedge mechanics.

The choice of the rheology is important for

modeling the deformation of the entire accretionary wedge, and Coulomb wedge models have proven to be successful in describing the wedge shape and overall mechanical behavior [1]. However, elastic deformation theory is used to describe sand-box models of accretionary wedges [6]. Here we want to draw a connection between the phenomenology of accretionary wedge deformation as observed in sand-box modeling and natural accretionary wedges. Therefore, we are using the same theoretical approach, namely elastic theory, for describing both cases, the natural accretionary wedge and the model.

Here, we apply elastic theory to an accretionary wedge to calculate the stress distribution in the wedge, closely following the work of Mandal et al. [6], and estimate the stress distribution along

* Corresponding author.

Tel.: +31-30-253-5076; Fax: +31-30-253-5030.

E-mail address: bert@geo.uu.nl (B. Schott).

an imbricate thrust and the sole thrust. This allows us to specify the conditions for the nucleation and propagation of a new imbricate thrust at the front of an accretionary wedge [9], without going into details of thrust initiation [10,11]. Although plastic rheology is significant in governing the style of deformation in an accretionary wedge, our elastic approach is a first approximation towards understanding the mode of initiation and propagation of an imbricate thrust in front of a shortening wedge.

Elastic theory applied to accretionary wedges together with high-resolution seismic cross-sections can be used to calculate relations between the coefficients of friction along frontal thrust faults and the basal décollement. However, theory usually focuses on a single fault and explicitly takes pore-fluid pressure into consideration [12], which is difficult to estimate.

Pore-fluid pressure is not explicitly taken into consideration in our equations, however, all coefficients of friction can be interpreted as being effective coefficients, having the weakening effect of pore-fluid pressure included. We do not consider the weakening of the décollement and low friction due to the presence of a ductile layer, which is the case in some fold/thrust belts (e.g. Zagros mountain belt and Salt Range [13,14]).

In Section 2 we will demonstrate that by assuming the equality of certain theoretical stress limits, an equation for the coefficient of basal friction can be derived, which is a function only of the wedge geometry and material properties. This theoretical treatment allows us to estimate the effective coefficient of basal friction ‘directly’ from high quality seismic cross-sections, which are available for many regions.

2. Estimating the coefficient of basal friction

To estimate the conditions for slip on a fault, we use an approach based on a force balance between the force driving slip and frictional resistance along an inclined fault [15]. These forces can be decomposed into vertical and horizontal components. These components of the forces can be calculated by vertically or horizontally integrating

over the respective components of the stress tensor, which are e.g. vertical lithostatic stress (σ_{zz}) and horizontal shortening stress (σ_{xx}). This approach was successfully applied to thrusting and used to derive an equation to describe imbricate thrust spacing in accretionary wedges [6]. We are building on this approach and show that the equations Mandal et al. [6] have derived can be used to estimate the coefficient of basal friction. Like Mandal et al. [6] we assume that the shortened sediment layer has a uniform initial thickness h_0 and the ‘wedge’ has a uniform thickness h_1 , neglecting any wedge shape. The length of the base of the wedge is b and the distance between the currently active fault and an incipient fault is a (Fig. 1). Because most of the deformation takes place in the vertical xz -plane, we assume plane strain conditions. An analysis of the stress field for such a model setup (Fig. 1) yields [6]:

$$\frac{s}{h} = \frac{\Sigma}{\mu_b \rho g h} + \frac{F(\vartheta, \mu, \mu_b)}{2\mu_b} \quad (1)$$

Eq. 1 relates the ratio of imbricate spacing s to layer thickness h to the shortening boundary stress Σ scaled by $\mu_b \rho g h$ and a function $F(\vartheta, \mu, \mu_b)$. The latter is defined as $F(\vartheta, \mu, \mu_b) = \mu_b / \tan(\vartheta) + G(\vartheta, \mu, \mu_b)$ for convenience, leading to $F < 0$ in our parameter range. Here, ρ is the density, g is the gravitational acceleration, ϑ is the dip of the fault, μ is the coefficient of friction along the fault, and μ_b is the coefficient of friction along the sole thrust. It is convenient to define the functions $G = (M(\vartheta, \mu) - \mu_b N(\vartheta, \mu)) / L(\vartheta, \mu)$, $L = -\sin(2\vartheta)/2 + \mu(\sin \vartheta)^2$, $M = \sin(2\vartheta)/2 + \mu(\cos \vartheta)^2$, and $N = \cos(2\vartheta) - \mu \sin(2\vartheta)$, which do not have a special physical meaning. Rearranging Eq. 1 shows that slip on the fault occurs if:

$$\frac{\Sigma}{\rho g} > \mu_b s - \frac{hF(\vartheta, \mu, \mu_b)}{2} \quad (2)$$

Eq. 2 can be applied to an already active frontal fault F_1 by setting $s = b$ and $h = h_1$ (Fig. 1) yielding:

$$\frac{\Sigma}{\rho g} > \mu_b b - \frac{h_1 F(\vartheta, \mu, \mu_b)}{2} \quad (3)$$

The formation of a new fault is geometrically similar to the above described slip along an existing fault in this model and therefore can theoretically be treated in the same way. Setting $\Sigma = \sigma_{xx}(x = x_0 = b)$, $s = a$, $h = h_0$, $\vartheta = \vartheta_i$, and $\mu = \mu_i$ gives us the horizontal stress at incipient fault F_2 :

$$\frac{\sigma_{xx}(b)}{\rho g} > \mu_b a - \frac{h_0 F(\vartheta_i, \mu_i, \mu_b)}{2} \quad (4)$$

The horizontal stress σ_{xx} decreases from the pushing boundary at $x = 0$ due to the basal friction and can be related to the push from the rear Σ by:

$$\frac{\sigma_{xx}(b)}{\rho g} = \frac{\Sigma}{\rho g} - \mu_b b \quad (5)$$

By solving Eq. 5 for Σ and inserting the result into Eq. 4 we can derive the lower limit of Σ :

$$\frac{\Sigma}{\rho g} > \mu_b(a + b) - \frac{h_0 F(\vartheta_i, \mu_i, \mu_b)}{2} \quad (6)$$

which must be reached before a new fault F_2 can form. When a new fault develops, the stress limits given by Eqs. 3 and 6 are equal. Assuming equality of the right hand sides of Eqs. 3 and 6, both equations can be combined to:

$$2a\mu_b = h_0 F(\vartheta_i, \mu_i, \mu_b) - h_1 F(\vartheta, \mu, \mu_b) \quad (7)$$

which can be solved for the coefficient of basal friction μ_b by re-substituting F , yielding:

$$\begin{aligned} \mu_b = & \left(h_0 \frac{M(\vartheta_i, \mu_i)}{L(\vartheta_i, \mu_i)} - h_1 \frac{M(\vartheta, \mu)}{L(\vartheta, \mu)} \right) \\ & \times \left(2a + \frac{h_1}{\tan(\vartheta)} - \frac{h_0}{\tan(\vartheta_i)} + h_0 \frac{N(\vartheta_i, \mu_i)}{L(\vartheta_i, \mu_i)} \right. \\ & \left. - h_1 \frac{N(\vartheta, \mu)}{L(\vartheta, \mu)} \right)^{-1} \quad (8) \end{aligned}$$

This expression for the coefficient of basal friction μ_b is a function of the fault and model geometry and the coefficients of friction μ_i and μ only. For typical parameters of a sand-box model of an accretionary wedge ($h_0 = 6.6$ mm, $\vartheta_i = 25^\circ$,

$\mu_i = 0.839$, $h_1 = 25.4$ mm, $\vartheta = 32^\circ$, $\mu = 0.35$, $a = 25$ mm) [9], the calculated value is $\mu_b \approx 0.28$, which is close to the experimentally found value of $\mu_b = 0.37$ [16], showing that our method can be used to estimate the coefficient of basal friction in such sand-box models.

3. Application to the Makran and Nankai accretionary wedges

Seismic images of the Makran [17] and the Nankai [18] accretionary wedge indicate the current formation of a new thrust (Fig. 1). In the top panel of Fig. 1 we show a seismic section across the Makran accretionary wedge with a line drawing overlaid. The simplified basal décollement is indicated by a white subhorizontal line (from A to B in Fig. 1) in about 8 km depth. The actual basal décollement (black line) departs from the straight line in the left and central part by approximately 500 m. The left incipient fault correlates with surface deformation and seismic reflectors, indicated by black lines. The right simplified active frontal fault is in its central part following the seismic reflector. The left vertical arrow indicates the undisturbed layer thickness h_0 , and the right vertical arrow indicates the shortened layer thickness h_1 used in the calculation.

In the middle panel of Fig. 1 we show a seismic section across the Nankai accretionary wedge with a line drawing overlaid. The simplified basal décollement is indicated by a gray subhorizontal line (from A to B in Fig. 1) between 5 and 5.7 km depth, which is almost perfectly following the actual basal décollement (black line, only visible left of the word ‘Décollement’). The left simplified active frontal fault is approximating the S-shaped fault plane found in the seismic section. The right incipient fault is assumed to either correlate with surface deformation and the left most inclined seismic reflector ($a = 2$ km), or with the indicated deformation front and the right most inclined seismic reflector ($a = 2.8$ km). The left vertical arrow indicates the shortened layer thickness h_1 , and the right vertical arrow indicates the undisturbed layer thickness h_0 used in the calculation.

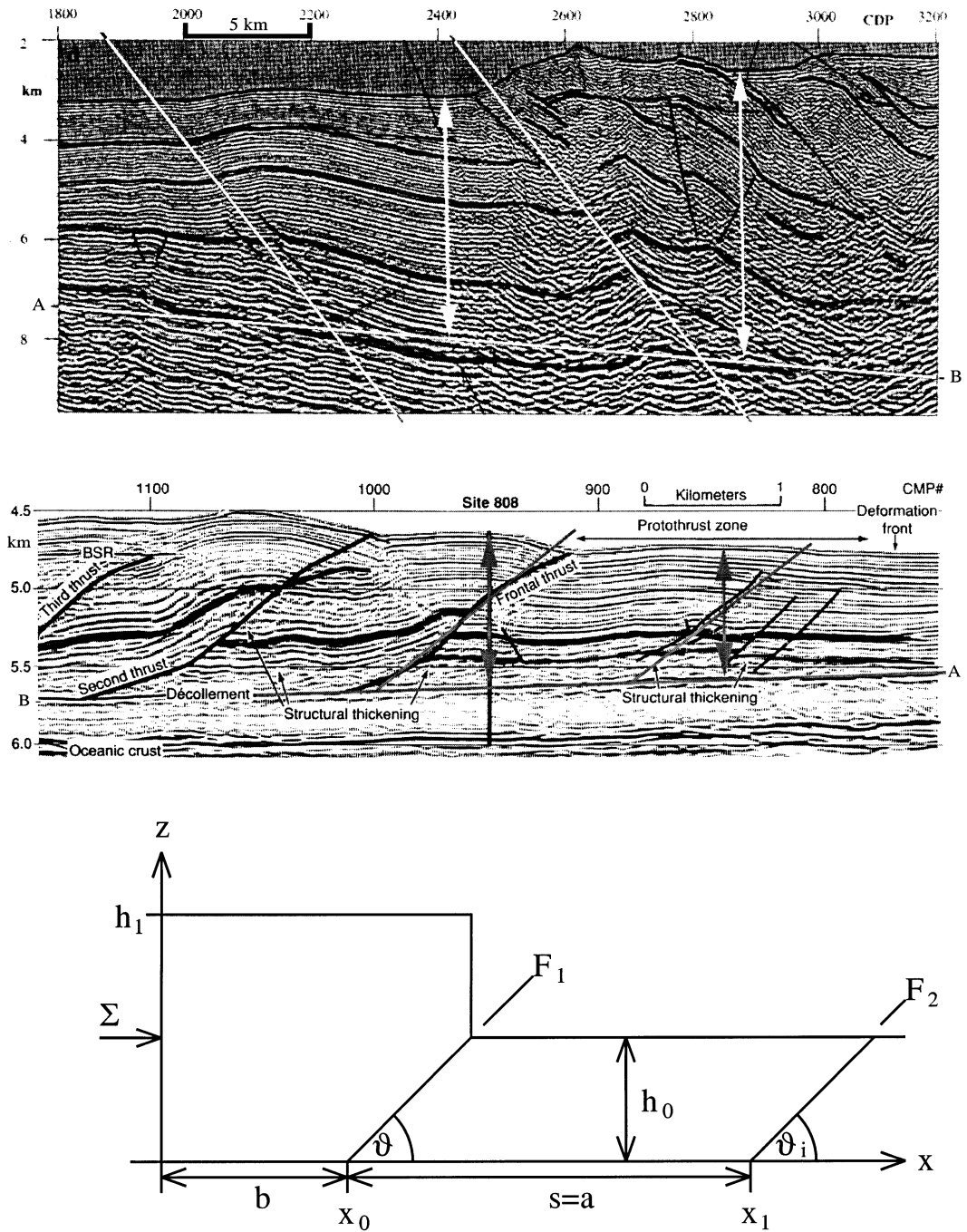


Fig. 1. Images of seismic sections across the Makran (top) and Nankai (middle) accretionary wedges, modified after [17,18]. The simplified basal décollement is indicated by a straight line from A to B, which is also indicating the orientation of subduction. A line drawing (bottom) indicates the simplified geometry of an accretionary wedge and the variables used for the theoretical analysis.

These seismic cross-sections allow us to estimate the coefficient of internal friction μ_i from the angle of fault formation ϑ_i by the relation $\mu_i = 1/\tan(2\vartheta_i)$. We will also assume that on an existing fault the coefficient of friction μ is less than the coefficient of internal friction μ_i ($\mu < \mu_i$), which is an upper limit approximation.

For the Makran accretionary wedge [17] we find $h_0 = 5$ km, $a = 14.5$ km, $\vartheta = 24^\circ$, and $h_1 = 5.7$ km and presume $\vartheta_i \approx 24^\circ$ and hence $\mu_i \approx 0.9$. We can now use Eq. 7 together with these parameters to calculate the coefficient of basal friction μ_b as a function of the coefficient of friction μ . However, the range of physically reasonable values is restricted to the domain where $\mu < \mu_i$, yielding $\mu_b \leq 0.2$ for the Makran accretionary wedge (Fig. 2).

The same procedure can be applied to the Nankai accretionary wedge [18], where we find $\vartheta_i \approx 31.3^\circ$ and hence $\mu_i \approx 0.52$. However, the location of the incipient fault is less clear, and its distance from the frontal fault is likely to be between $a = 2$ km and $a = 2.8$ km. The other parameters are $h_0 = 0.86$ km, $\vartheta = 38^\circ$, and $h_1 = 1$ km. We use again Eq. 7 together with these parameters to calculate $\mu_b(\mu)$ and find $\mu_b \leq 0.1\text{--}0.16$ for $\mu < \mu_i$

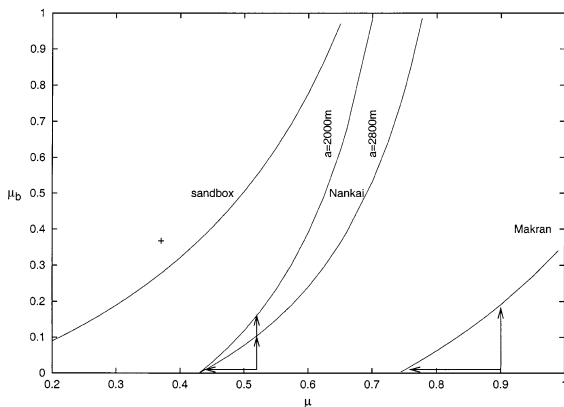


Fig. 2. Coefficient of basal friction μ_b as a function of μ for a sand-box model of an accretionary wedge, and for the Nankai and Makran accretionary wedges. An experimentally found data point for the sand-box model is indicated by a plus sign (+). For the accretionary wedges the ranges of possible values of the friction coefficients μ and μ_b are indicated by arrows.

for the Nankai accretionary wedge, and for a fault spacing of $a = 2\text{--}2.8$ km (Fig. 2).

This calculation results in roughly the same upper limits of the coefficient of basal friction $\mu_b(\mu)$ for both accretionary wedges, which is not surprising, because both show a similar mode of deformation, with a thrust spacing to layer thickness ratio of either $s/h \approx 1$ (Makran) or $s/h \approx 2$ (Nankai) (Fig. 1).

4. Conclusions and discussion

The elastic theory of faulting (e.g. [15]) can be used to understand imbricate thrust spacing [6]. This approach also allows us to estimate the stress limit, which must be reached for the development of a new fault in front of an accretionary wedge (Eq. 6). When the horizontal stress along the youngest and most active imbricate surface within an accretionary wedge (frontal fault) reaches a critical limit, the sole thrust propagates forward and a new imbricate steps up (incipient fault) [9].

The stresses at the frontal and the incipient fault can be related to each other in this particular situation (Eqs. 3 and 6) and allow us to estimate the coefficient of basal friction in accretionary wedges from geometrical parameters such as fault dip ϑ , thrust spacing a , and layer thickness h , and material properties such as coefficient of (internal) friction μ (μ_i) and density ρ (Eq. 7), which can be measured from seismic cross-sections or be estimated, respectively (Fig. 1).

Our calculated upper limits for the coefficient of basal friction for the Makran ($s/h \approx 1$) and Nankai ($s/h \approx 2$) accretionary wedges are $\mu_b \approx 0.2$ and $\mu_b \approx 0.1\text{--}0.16$, respectively. The relative magnitude of these values is correct according to the theoretical proportionality $s/h \sim 1/\mu_b$ from Eq. 1. These values may appear to be too low, however, they must be interpreted as effective coefficients of basal friction, because we do not explicitly take the effect of pore-fluid pressure into consideration.

Assuming $\mu_{b,dry} = 0.85$ for dry conditions and $\lambda = 0.98$ for Makran and $\lambda = 0.5$ for Japan [1], the effective coefficients of basal friction are

$\mu_b = (1-\lambda)\mu_{b,dry} = 0.02 \cdot 0.85 \approx 0.017$ and $\mu_b = (1-\lambda)\mu_{b,dry} = 0.5 \cdot 0.85 \approx 0.425$ for Makran and Nankai, respectively (λ is the ratio of pore fluid to lithostatic pressure).

The effective coefficient of basal friction $\mu_b \approx 0.017$ calculated for Makran by Davis et al. [1] is less than the upper limit of $\mu_b \approx 0.2$ derived in this study. Such a low coefficient of basal friction requires a relatively low coefficient of friction $\mu < 0.75$ on existing faults, which is not unlikely according to our results (Fig. 2).

The effective coefficient of basal friction $\mu_b \approx 0.425$ calculated for Nankai from the assumptions by Davis et al. [1] is much higher than the upper limit of $\mu_b \approx 0.1$ – 0.16 derived in this study. Such a high coefficient of basal friction would be close to the coefficient of internal deformation $\mu_i \approx 0.52$ found from the angle of fault initiation, and favors a very small imbricate spacing to layer thickness ratio $s/h < 1$ and a very steep wedge slope [19], given that the results from analogue modeling of accretionary wedges can be applied to nature. However, such a high coefficient of basal friction is unlikely for the Nankai accretionary prism, where the thrust spacing to layer thickness ratio s/h is not less than one, but is $s/h \approx 2$, which can be directly taken from the seismic cross-section provided in Fig. 1. Therefore, our estimate of the upper limit of $\mu_b \approx 0.1$ – 0.16 is more consistent with the observed thrust spacing.

A low effective coefficient of basal friction between $\mu_b = 0.05$ and $\mu_b = 0.09$ was suggested for Nankai based on force balance and finite element modeling [20]. The corresponding effective coefficient of friction along thrust faults would be $\mu \approx 0.48$ according to our results (Fig. 2), which is slightly less than the coefficient of internal friction for the formation of a new fault. Hence, this is a reasonable value for μ on an existing fault plane, and shows that our method would estimate the coefficients of friction in the same range.

A comparison of the results from this simplified approach to results from a more complicated approach, in which the wedge shape is considered, shows that both approaches predict the same thrust spacing s as a function of the layer thickness h in situations of low compressive stress [6].

Such low-stress conditions are reported for the Nankai accretionary wedge [20].

Acknowledgements

Thanks are due to Genene Mulugeta and Chris Talbot for stimulating discussion. This article benefited from the thorough and very constructive review by Kelin Wang. One anonymous reviewer is acknowledged for his critical review and a second one for his final review. This paper also profited from valuable discussion with Rob Govers. H.A.K. is funded by the Swedish Natural Sciences Research Council (NFR) and B.S. was supported by NFR Post-Doc Grant G-AA/GU 09843-325.[AC]

References

- [1] D. Davis, J. Suppe, F.A. Dahlen, Mechanics of fold-and-thrust belts and accretionary wedges, *J. Geophys. Res.* 88 (1983) 1153–1172.
- [2] R.C. Fletcher, Approximate analytical solutions for a cohesive fold-and-thrust wedge: some results for lateral variation in wedge properties and for finite wedge angle, *J. Geophys. Res.* 94 (1989) 10347–10354.
- [3] F.A. Dahlen, Noncohesive critical coulomb wedges: An exact solution, *J. Geophys. Res.* 89 (1984) 10125–10133.
- [4] F.A. Dahlen, J. Suppe, D.M. Davis, Mechanics of fold and-thrust belts and accretionary wedges (continued): cohesive coulomb theory, *J. Geophys. Res.* 89 (1984) 10087–10101.
- [5] A. Yin, Mechanics of wedge-shaped fault blocks 1. An elastic solution for compressional wedges, *J. Geophys. Res.* 98 (1993) 14245–14256.
- [6] N. Mandal, A. Chattopadhyay, S. Bose, Imbricate thrust spacing: experimental and theoretical analyses, in: S. Sen Gupta (Ed.), *Evolution of Geological Structures in Micro to Macro-scales*, Chapter 8.1, Chapman and Hall, London, 1997.
- [7] W.M. Chapple, Mechanics of thin-skinned fold-and-thrust belts, *Geol. Soc. Am. Bull.* 89 (1978) 1189–1198.
- [8] G.S. Stockmal, Modeling of large-scale accretionary wedge deformation, *J. Geophys. Res.* 88 (1983) 8271–8287.
- [9] H.A. Koyi, B. Schott, Stress estimations from fault geometries applied to sand-box accretionary wedges, *Geophys. Res. Lett.* 28 (2001) 1087–1090.
- [10] J. Panian, W. Pilant, A possible explanation for foreland thrust propagation, *J. Geophys. Res.* 95 (1990) 8607–8615.

- [11] D. Goff, D.V. Wiltschko, Stresses beneath a ramping thrust sheet, *J. Struct. Geol.* 14 (1992) 437–449.
- [12] D.M. Davis, R. v. Huene, Inferences on sediment strength and fault friction from structures at the Aleutian Trench, *Geology* 15 (1987) 517–522.
- [13] D. Davis, T. Engelder, The role of salt in fold-and-thrust belts, *Tectonophysics* 119 (1985) 67–88.
- [14] C.J. Talbot, M. Alavi, The past of a future syntaxis across the Zagros, in: *Salt Tectonics*, Geol. Soc. London Special Publ. 100 (1995) 89–110.
- [15] D.L. Turcotte, G. Schubert, *Geodynamics: Applications of Continuum Physics to Geological Problems*, 1st edn., John Wiley and Sons, New York, 1982, 450 pp.
- [16] G. Mulugeta, Modeling the geometry of Coulomb thrust wedges, *J. Struct. Geol.* 10 (1988) 847–859.
- [17] J. Fruehn, R.S. White, T.A. Minshull, Internal deformation and compaction of the Makran accretionary wedge, *Terra Nova* 9 (1997) 101–104.
- [18] G.F. Moore, D.E. Karig, T.H. Shipley, A. Taira, P.L. Stoffa, W.T. Wood, 2. Structural framework of the ODP LEG 131 area, Nankai Trough, in: *Proceedings of the Ocean Drilling Program, Initial Reports*, 131, 1991, pp. 15–20.
- [19] G. Mulugeta, Squeeze box in a centrifuge, *Tectonophysics* 148 (1988) 323–335.
- [20] K. Wang, J. He, Mechanics of low-stress forearcs: Nankai and Cascadia, *J. Geophys. Res.* 104 (1999) 15191–15205.